



Contents lists available at ScienceDirect

Gondwana Research

journal homepage: www.elsevier.com/locate/gr

Severe selenium depletion in the Phanerozoic oceans as a factor in three global mass extinction events

John A. Long^{a,b,*}, Ross R. Large^c, Michael S.Y. Lee^{d,e}, Michael J. Benton^f, Leonid V. Danyushevsky^c, Luis M. Chiappe^g, Jacqueline A. Halpin^c, David Cantrill^h, Bernd Lottermoser^{c,i}

^a School of Biological Sciences, Flinders University, POB 2100, Adelaide, SA 5001, Australia

^b Museum Victoria, PO Box 666, Melbourne, VIC 3001, Australia

^c ARC Centre of Excellence in Ore Deposits (CODES), School of Physical Sciences, University of Tasmania, Private Bag 79, Hobart Tasmania, 7001, Australia

^d South Australian Museum, North Terrace, Adelaide, SA 5000, Australia

^e School of Earth and Environmental Sciences, The University of Adelaide, SA 5005, Australia

^f School of Earth Sciences, University of Bristol, Bristol BS8 1RJ, UK

^g The Natural History Museum of Los Angeles County, 900 Exposition Blvd, Los Angeles, CA 90007, USA

^h Royal Botanic Gardens Victoria, Melbourne, VIC 3004, Australia

ⁱ Institute of Mining Engineering, RWTH Aachen University, Aachen, Germany

ARTICLE INFO

Article history:

Received 4 September 2015

Received in revised form 6 October 2015

Accepted 6 October 2015

Available online xxxx

Handling Editor: M. Santosh

Keywords:

Trace elements

Geochemistry

Oceans

Mass extinctions

ABSTRACT

Selenium (Se) is one of the key trace elements required by all animal and most plant life, and Se deficiencies in the food chain cause pathologies or death. Here we show from new geochemical analyses of trace elements in Phanerozoic marine pyrite that sustained periods of severe Se depletion in the past oceans correlate closely with three major mass extinction events, at the end of the Ordovician, Devonian and Triassic periods. These represent periods of Se depletion >1.5–2 orders of magnitude lower than current ocean abundances, being within the range to cause severe pathological damage in extant Se-reliant organisms. Se depletion may have been one of several factors in these complex extinction scenarios. Recovery from the depletion/extinction events is likely part of a natural marine cycle, although rapid rises in global oxygen from sudden major increases in marine productivity and plant biomass after each extinction event may also have played a crucial role.

© 2015 International Association for Gondwana Research. Published by Elsevier B.V. All rights reserved.

1. Introduction

Many trace elements (TEs) are essential for the formation and sustainability of life (Mertz, 1957; Klasing, 1998; Eisler, 2000). In this study we use a new dataset of TE abundances in past oceans (Large et al., 2014; Large et al., 2015a), to discuss whether three of the five Phanerozoic mass extinction events could have been influenced by extreme low abundances in the trace element selenium (Se).

New laser ablation-inductively coupled plasma mass spectrometry (LA-ICPMS) techniques have been used to measure such TE with accuracy down to single parts per billion in pyrite from marine black shales (Large et al., 2014). This dataset of TE throughout the past 3.5 billion years, based initially on some 1885 pyrite analyses (Large et al., 2014), and now updated to include over 2200 analyses for the Late Neoproterozoic–Phanerozoic (Large et al., 2015a) has revealed that essential TEs in the oceans fell below critical thresholds during three

mass extinction events at the end of the Ordovician, Devonian and Triassic. Mechanisms for these extinction events are debated, although scenarios for these events involve global climate change associated with widespread anoxia and eustatic sea level changes (Ordovician, Devonian) as well as the Central Atlantic Magmatic Province (CAMP) eruptions (Triassic) (Table 1). Here we present the evidence based on known environmental and tolerance levels of Se in a range of extant organisms from phytoplankton to vertebrates to propose how distinct periods of severe Se depletion in past oceans offer a potential new causal factor in these mass extinction events.

1.1. Selenium, weathering and oceans

Se, a naturally occurring metalloid, is unique in that although it is an essential micronutrient in most organisms, including bacteria, archaea, fish and shellfish, it may be toxic at high concentrations and has a very narrow concentration window for sustaining marine life, as discussed further below. The Se content of the crust averages 0.05 ppm, with the highest levels found in shales (up to 675 ppm), coals (up to 20 ppm) and volcanic tuffs (up to 9.2 ppm), compared with igneous rocks that

* Corresponding author at: School of Biological Sciences, Flinders University, POB 2100, Adelaide, South Australia, Australia 5001.

E-mail address: john.long@flinders.edu.au (J.A. Long).

Table 1 Major Phanerozoic mass extinction events. Summarises main evidence and most plausible hypothesis explaining the five major mass extinction events with comments on levels of trace element abundance in the oceans at these times.

Extinction event	Most accepted causes	Evidence	Comments	TE abundance in oceans
End Ordovician (443 Mya) c. 85% marine species lost	South Pole glaciation, eustatic sea level changes and cooling caused 1st pulse, widespread anoxia, caused 2nd pulse.	Gondwana glacial deposits; $d^{13}C$, $d^{18}O$ trends;	High CO_2 levels; lower O_2 levels (50% current oceanic levels; major increase in plant diversity immediately after event, plants invade land habitats)	Severe Se deficiency over 8 My period before extinction event
End Devonian (Frasnian–Famennian, 370–372 Mya) Between 13 and 40% families, 50–60% genera lost	(1) Anoxia, eustatic sea-level changes, epicontinental seas invaded by anoxic waters. (2) Large bolide impact	(1) Kellwasser event layers indicate widespread anoxia, 2 pulses before Frasnian–Famennian boundary; $d^{13}C$, $d^{18}O$ trends (2) Sijian Crater and others. Ir anomaly	(1) Extinctions only recorded in marine habitats; no change to terrestrial land flora (2) Timing of impacts to extinctions not well constrained	Severe Se deficiency in 2 pulses in 16–18 My period before end-Devonian; other TEs show that severe deficiencies in staged order (Co, Cu to 380 Mya) would affect all life requiring Se
End Devonian (Hangenberg, 359 Mya) Between 16% families, 21% genera lost; 50% vertebrate diversity lost	Global climate changes (cooling); sea level drop, eutrophication, anoxia.	Glacial deposits central USA, China, Europe, South America; $d^{13}C$, $d^{18}O$, $^{87}Sr/^{86}Sr$ trends Brezinski et al., 2008 (palaeox. 3268: 143–151)	Fauna that survived end Frasnian event much depauperate; on land major increase in land plant biomass and extent during Late Devonian; no major land plant extinctions across DC boundary	Severe Se depletion at end Devonian, along with severe Mo deficiency 370–360 Mya would affect all marine life requiring Se and Mo.
End Permian (251 Mya) Between 80 and 94% all species lost	(1) Massive volcanic activity and subsequent effects on terrestrial and marine ecosystems (2) Bolide impact	(1) Siberian traps dated 251 Myr; $d^{13}C$, $d^{18}O$ trends;	High CO_2 levels; impact evidence unreliable (Benton and Twitchett, 2003)	No significant change in oceanic TE levels
End Triassic (201 Mya) c. 50% marine species lost	Massive volcanic activity, acidification in oceans, anoxia	Central Atlantic Magmatic Province deposits; Long chain n-alkanes in plants; negative $d^{13}C_{org}$ excursion	Major vegetative turnover; High CO_2 levels; terrestrial extinctions not as dramatic (not well accounted for)	Severe Se deficiency would affect all marine life requiring Se
End Cretaceous (66 Mya) c. 60% species lost	Large bolide impact	Chicxulub Crater, impact ejecta, Ir layer.	Timing of actual extinctions in relation to impact event.	No significant change in oceanic TE levels

range from 0.01 to <2 ppm (Plant et al., 2005). Cretaceous organic-bearing chalks are also reported to contain up to 70 ppm Se (Kulp and Pratt, 2004).

Selenium has multiple oxidation states -2 , 0 , $+4$ and $+6$. Under oxic geological conditions selenate (Se^{6+}) is the predominant inorganic species; under suboxic conditions selenite (Se^{4+}) is predominant, but in anoxic to euxinic environments selenide (Se^{2-}), organo-Se complexes and elemental Se^0 are most stable. Both selenite and selenate are highly soluble, but selenite is readily absorbed onto iron oxides and organic matter, especially in low pH environments, leading to its retention in the soil profile under favourable conditions (Neal et al., 1987). Consequently, selenite is less bioavailable than selenate (Fordyce, 2007). Oxidation of Se^{4+} to Se^{6+} enhances Se mobility and persistence in natural waters.

The principal crustal weathering source of selenium is disseminated pyrite in sedimentary and volcanic rocks where the Se substitutes for S in the structure of pyrite. Sedimentary pyrite contains from <0.5 to 5209 ppm Se with an arithmetic mean of 145 ppm (Large et al., 2015a). Oxidative weathering of pyrite leads to the release of selenium as both the selenate and selenite species. Under neutral to alkaline conditions the selenate species remains highly soluble, where it can be readily transported via river systems to the ocean (Cutter, 1989). Under reduced conditions, continental weathering releases little soluble Se, as the selenide, elemental Se^0 and organo-selenium complexes are relatively insoluble (Kulp and Pratt, 2004). Thus, significant increases in atmospheric oxygen, accompanied by active erosion, can lead to a major increase in the supply of soluble Se to the ocean. The degree of oxidation and pH controls the selenate to selenite ratio of the released selenium, which in turn controls the Se solubility in surface run-off, and consequently the amount of Se which is delivered to the oceans, other factors remaining constant. Studies of dissolved TE supply from rivers to the ocean (Kharkar et al., 1968) indicate that Se has a narrow concentration range, similar to Ag, Co, Rb and Cs and in contrast to Mo, Cr and Sb, which show extremely large variations from river to river. This study also showed that most of the stream load of Se was dissolved, with only 10% adsorbed onto particles, which became desorbed on contact with seawater.

In the marine environment three species are present, selenite, selenate and a form of organic selenides (Cutter and Bruland, 1984). Selenite is supplied from decomposition of selenite-silicate compounds in the hard tissues of phytoplankton in the tropical and subtropical parts of the Pacific Ocean (Nakaguchi et al., 2008). Organic selenides (seleno-amino acids in complex peptides) dominate surface waters down to about 200 m, below which selenate and selenite are the major dissolved species (Cutter and Cutter, 1995). The low concentration of dissolved oxidised Se in the upper ocean layers is due to biochemical reduction of the oxidised species into labile organic particulates during assimilation by marine organisms, which sink, die and dissolve, consequently regenerating the dissolved selenate and selenite species at lower ocean levels, typical of a nutrient profile. In the deep ocean the oxidised Se species are reduced to Se^0 or HSe^- , and incorporated into pyrite (Mitchell et al., 2012). A small fraction of the organically fixed selenium eventually deposits in seafloor muds (Herring, 1991). Ryser et al. (2005) showed that Se in black shale is present as anaerobic microbial respiration products resulting from microbial reduction of Se oxyanions; including Se-substituted for S in pyrite, di-selenide carbon compounds and dzharkenite ($FeSe_2$; an isometric polymorph of ferroselite). Experimental studies (Diener et al., 2012) indicate that Se^{2-} in solution is taken up (98%) by pyrite to produce a $FeSSe$ compound with a slightly distorted pyrite structure. Ferroselite ($FeSe_2$) has also been produced by reacting nanoparticles of pyrite and greigite with selenite and selenate bearing solutions (Charlet et al., 2012). Our LA-ICPMS imaging of pyrite in black shales of various metamorphic grades indicates that pyrite is considerably enriched in Se compared with the clay-rich and organic-rich matrices. Our analytical data indicate that Se in pyrite is enriched, on average, 5.8 times over the Se

Table 2
LA-ICPMS trace element data (from Large et al., 2015a).

Sample Age (Ma)	Mn (ppm)	Co (ppm)	Ni (ppm)	Cu (ppm)	Zn (ppm)	Se (ppm)	Mo (ppm)	Cd (ppm)
0.1	2238.19	39.74	363.11	280.39	538.46	132.47	479.07	11.57
53	414.19	160.24	104.16	264.87	261.25	46.09	211.84	5.42
56	220.95	95.74	261.63	545.28	342.93	58.42	185.98	2.32
83	297.54	37.51	135.72	214.96	35.18	4.13	2.52	0.43
91	14.54	220.21	528.46	121.64	13.39	10.42	8.52	0.12
92	14.03	171.21	495.82	109.77	8.96	3.54	8.65	0.08
125	440.12	36.74	73.80	289.10	159.19	25.57	130.96	0.17
131	27.60	8.82	35.71	5.34	17.87	3.24	25.83	1.56
142	109.31	50.64	283.56	79.78	42.46	5.92	10.04	0.16
145	38.55	159.67	455.64	61.95	17.51	4.63	7.00	bd
169	11.28	107.23	251.88	4.95	4.32	2.13	13.65	2.11
180	50.07	33.95	187.24	48.59	12.54	11.17	95.66	0.54
190	865.02	238.55	287.47	76.93	47.91	1.52	18.41	0.06
202	4.67	25.63	157.35	42.14	5.45	1.82	32.15	0.03
205	239.71	7.32	338.88	285.88	58.12	62.57	11.29	2.77
230	bd	267.65	107.96	464.27	1093.35	6.50	4.21	0.62
235	8.87	1372.33	360.15	398.48	139.03	60.98	30.87	1.52
250	1093.93	1017.08	255.82	1107.78	3399.74	8.48	19.15	2.17
251	411.74	79.20	111.13	139.31	73.90	10.47	44.40	1.74
253	30.50	249.36	708.70	143.57	16.59	22.38	17.49	0.52
272	814.94	32.77	1088.44	499.53	835.38	1259.03	819.30	85.65
285	15.95	204.17	275.18	1.54	6.13	18.92	27.48	0.81
297	14.76	90.74	166.82	25.20	8.35	19.17	4.47	0.14
305	538.01	59.45	3262.73	180.68	2104.11	328.29	1886.80	74.15
310	515.38	85.03	2290.85	542.28	1630.65	1347.39	630.39	25.41
328	594.25	7.34	1466.84	1390.71	2919.58	2400.78	324.73	283.85
331	520.52	41.71	312.96	41.00	14.42	18.04	57.40	1.18
332	898.54	86.85	240.65	48.48	122.66	10.38	8.98	1.09
333	19.72	6.42	344.89	177.61	5.25	235.78	125.89	4.27
338	78.90	202.39	346.70	253.08	13.27	6.20	0.62	0.75
339	34.65	493.92	1029.19	715.25	11.27	6.47	1.65	0.41
340	438.20	238.12	353.53	647.27	43.37	9.89	12.40	1.80
349	277.73	119.94	208.65	105.69	10.84	4.60	7.26	1.46
350	387.48	184.52	1053.59	497.43	43.35	22.57	12.63	0.22
352	1493.86	195.96	572.98	475.63	186.26	17.86	15.59	1.06
355	275.69	68.50	323.17	242.15	34.70	53.81	123.81	2.01
356	327.38	407.35	418.54	273.98	87.50	5.35	2.41	1.20
357	88.86	457.92	1249.90	228.94	30.74	4.08	9.33	0.31
359	244.41	472.99	309.17	203.23	169.78	4.65	1.00	0.16
365	1622.16	137.53	225.56	260.75	155.98	7.30	83.00	0.50
366	248.22	179.80	111.82	61.64	149.32	10.79	3.80	0.53
367	277.97	610.97	787.50	389.75	63.80	1.76	4.72	1.40
368	482.90	311.90	248.82	177.39	116.36	8.22	6.02	0.47
370	596.70	338.26	184.37	144.18	99.57	3.58	9.02	0.41
375	453.09	193.25	499.84	174.24	85.75	20.25	25.52	0.86
376	773.46	113.16	276.49	119.29	289.13	20.07	30.71	5.52
377	160.14	262.01	943.94	611.85	109.76	52.28	29.78	1.11
378	69.77	133.58	601.47	237.57	30.43	21.39	35.43	1.05
379	277.17	343.42	1320.83	189.31	38.24	22.75	19.74	0.72
380	158.15	303.42	842.16	247.93	47.84	25.73	33.17	0.88
381	138.70	15.20	122.42	192.47	5.17	18.65	4.11	0.38
382	19.63	60.83	811.52	176.83	10.72	173.08	24.80	3.12
383	216.05	257.33	249.08	239.46	12.74	11.56	12.97	0.85
384	13.90	17.00	108.38	42.06	22.65	78.45	23.39	1.10
385	20.37	15.88	122.43	45.49	12.10	110.51	32.26	1.51
386	10.70	8.15	83.26	35.85	14.82	45.89	32.19	0.90
387	7.62	3.53	268.83	159.03	24.95	168.75	25.39	2.83
388	207.72	29.83	258.62	244.91	51.98	80.90	20.16	2.62
390	1402.97	1.07	281.52	1111.56	101.37	1381.37	333.16	12.54
393	56.70	312.57	434.97	57.29	8.19	4.98	25.58	0.12
395	1111.76	1.15	230.59	312.57	105.09	298.96	18.51	2.00
400	868.60	0.62	215.54	274.46	151.45	183.30	14.16	2.35
410	45.97	73.82	108.99	34.08	10.57	25.18	26.48	1.66
415	160.59	5.28	526.16	178.34	108.85	109.94	258.98	10.11
416	3676.46	134.49	1119.55	922.45	307.35	91.29	106.38	2.94
418	38.24	3.54	224.20	10.04	3.21	9.30	19.95	0.39
420	369.14	75.39	947.32	276.44	114.88	114.47	180.05	7.49
444	1307.83	25.46	247.14	325.05	115.19	56.49	281.58	5.23
450	810.18	133.33	745.33	462.43	320.98	3.16	48.67	1.41
455	27.08	29.19	331.63	367.60	27.24	1.64	10.53	0.35
456	3.96	18.12	268.87	56.27	2.91	2.60	2.50	0.15
457	2.65	112.30	553.19	32.46	1.97	2.20	2.03	0.15
458	213.63	66.40	496.37	98.40	161.74	12.50	33.61	0.50

(continued on next page)

Table 2 (continued)

Sample Age (Ma)	Mn (ppm)	Co (ppm)	Ni (ppm)	Cu (ppm)	Zn (ppm)	Se (ppm)	Mo (ppm)	Cd (ppm)
459	2.82	17.97	151.69	150.38	16.61	3.11	14.38	0.28
463	5.25	1.46	17.15	29.21	10.56	1.93	6.04	0.55
470	17.89	505.07	567.43	120.72	15.95	41.75	1.61	0.36
490	144.48	88.22	2425.44	397.66	45.64	88.89	27.54	3.33
500	12.97	131.29	362.56	240.43	57.54	109.99	3.19	1.26
510	1443.41	19.33	762.69	2226.45	540.25	366.32	358.11	14.16
523	622.37	3.52	884.62	141.97	78.72	547.65	3235.55	0.76
540	122.71	122.40	713.00	744.13	18.51	62.71	4.47	0.47
550	486.28	35.32	482.85	369.64	39.96	322.99	278.67	13.12
555	759.77	645.03	568.54	1319.73	22.88	10.62	4.35	0.96
560	353.85	330.56	869.15	589.39	201.67	9.20	8.77	1.45

bd = below detection

content of the black shale matrix (which commonly contains microscopic grains of pyrite). This compares with Mo, which is only enriched 2.5 times relative to the matrix.

2. Analytical methods

2.1. Trace element analysis

Trace element analysis of sedimentary pyrite was performed using LA-ICPMS. All analyses were conducted at the ARC Centre of Excellence in Ore Deposits (CODES), University of Tasmania. Instrumentation used involved a 213 nm solid-state laser microprobe (UP213, New Wave Research) coupled to an Agilent 7500a quadrupole mass-spectrometer, and a 193 nm solid-state laser microprobe (UP193ss, New Wave Research) coupled to Agilent 7700 s quadrupole mass-spectrometer. Laser microprobes are equipped with custom-made constant-geometry ablation cells. The proof of concept paper demonstrating how this method works, detailing exact methods used and quality of TE data collected is discussed in Large et al. (2014) and this is further discussed in Large et al. (2015a,b). Locations of the 182 black shale samples and individual pyrite analyses used in this research are given in the Supplementary information of Large et al. (2015a) and the Phanerozoic data are reproduced here as Table 2. All samples are black carbonaceous shales containing from 1 wt.% to 15 wt.% pyrite. The pyrite commonly formed under variable anoxic to euxinic water columns, principally in continental margin marine environments. Detailed sedimentological environmental data necessary for precise definition of the tectonic/sedimentary setting of each sample is not available.

2.2. Determining selenium levels in Phanerozoic oceans

Levels of Se in the current oceans are between 60 and 120 ppt in surface water, and 200 ppt in deep waters (Sugimura et al., 1976). TE level in seawater is robustly correlated with TE abundance in pyrite, based on samples forming in the Cariaco Basin in Venezuela (Large et al., 2015a). Based on current Se levels in seawater of 155 ppt (<http://www.mbari.org/chemsensor/summary.html>) and the pyrite dataset presented in Large et al. (2015a), which yields a geometric mean for Se in modern pyrite from the Cariaco Basin (0.1 Ma) of 132 ppm ($n = 92$), the following relationship can be generated:

$$\text{Seawater Se ppt} = (\text{pyrite Se ppm})/0.85.$$

This is a first order relationship that is unlikely to apply to all marine environments at all periods of ocean history. However it is the best estimate available and is applicable to continental margin basins in the Phanerozoic, which is the dominant environment sampled in this study.

2.3. Selenium tolerance levels in extant organisms

Se is an essential TE for all animal life utilised in the formation of necessary anti-oxidising enzymes and selenoproteins. A selenium cycle involving bacteria, fungi and higher plants metabolising selenite and selenate was first proposed by Shrift (1964). Although not essential for plant growth, low concentrations improve growth, and some obligate plants hyperaccumulate Se with dry tissue containing from 1000 to 10,000 ppm (Fan and Kizer, 1990). Se is utilised in the formation of the anti-oxidising enzymes glutathione peroxidase and thioredoxin reductase. Selenocysteine, an amino acid containing Se, is found in both eukaryotes and prokaryotes, with aquatic organisms having larger and more Se-dependent selenoproteomes, and in particular all vertebrates, both terrestrial and aquatic, have large selenoproteomes (Thisse et al., 2003; Lobanov et al., 2007). Se can be used to accelerate growth in higher organisms, such as in sea bream larvae fed on Se-enriched rotifers (Kim et al., 2014). Se, however, is toxic if ingested in concentrations greater than 5 ppm per day, and if livestock ingest plants containing 20–50 ppm this causes 'alkali disease' an acute form of Se poisoning (Fan and Kizer, 1990). In high doses Se can also cause carcinostatic activity (Spallholz, 1994).

Dissolved organic selenides account for nearly 80% of dissolved Se in the uppermost levels of seawater and represent the source of Se for phytoplankton (Price and Harrison, 1988), of which 89% of oceanic diatom species require Se (Harrison et al., 1988). Within the food chain this in turn accounts for a large number of selenoproteins occurring in algae and fishes. Plankton cultures deprived of Se in seawater for >5 days did not recover even when Se was added afterwards (Fig. 1; Harrison et al., 1988). The study concluded that it was more difficult for these Se-dependent microorganisms to recover after exposure to Se depletion than from exposure to nitrogen or phosphorus limitation. Similar results are found in Doblin et al. (1999) where three phytoplankton species (*Gymnodinium catenatum*, *Alexandrium minutum*, *Chaetoceros* cf. *tenuissimus*) showed rapid decline in Se deficient seawater, resulting in cessation of cell division after eight weeks of Se depletion. Many other studies confirm the dependency of plankton on minimal levels of Se in seawater (e.g. Wheeler et al., 1982; Keller et al., 1984; Price et al., 1987).

Se, thus, has a narrow margin of tolerance in biological systems (Fan and Kizer, 1990; Wang et al., 2012). Se levels at, or lower than, two orders of magnitude relative to current levels in current seawater strongly retard phytoplankton growth (Harrison et al., 1988). Se requirements in molluscs and fishes indicate lower limits for healthy growth that vary by one or two orders of magnitude (Hilton et al., 1980; Hamilton, 2004; Wang et al., 2012). Molluscs, such as abalone, have ingestion ranges for Se tolerance around 1.4–9 ppm (Wang et al., 2012) and fishes have Se tolerance ranges from 0.15 to 0.38 ppm (trout, Hilton et al., 1980) to 7 ppm (juvenile grouper, Lin and Shai, 2005). These data are summarised in Fig. 1 and form the basis of our interpretation of past

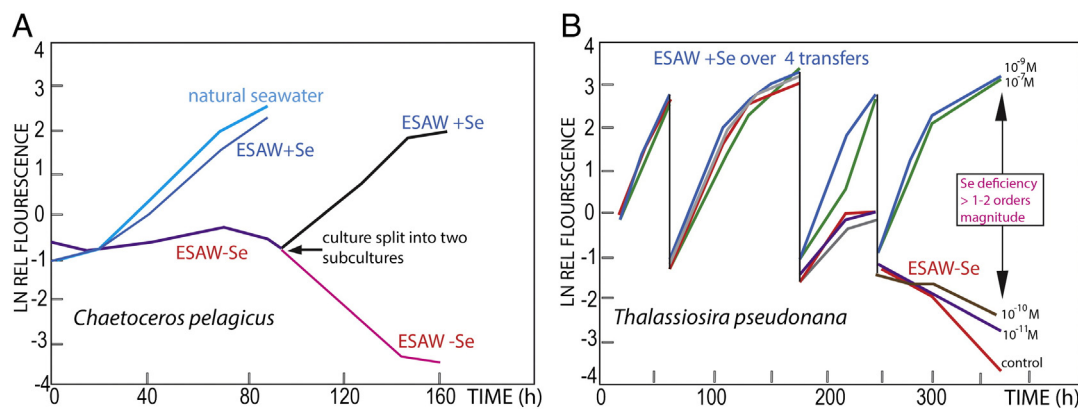


Fig. 1. Selenium deficiency in two common taxa of phytoplankton (diatoms, A, *Chaetoceros*; B, *Thalassiosira*), with transfers of subcultures from artificial seawater (ESAW) with Se added to artificial seawater with Se depleted. Note dramatic decrease after 250 h if threshold level for minimum selenium drops by 1–2 orders of magnitude for *Thalassiosira pseudonana*. From Harrison et al. (1988).

oceanic levels reaching critically low in Se levels. We postulate that extreme levels of Se deficiency in the oceans in past times would have stressed a high proportion of the biota dependent upon Se, making them unable to make sufficient vital selenoproteins and enzymes. It is, however, difficult to quantify the exact magnitude of this effect on the marine food chain without more detailed taxon-specific knowledge about organismal tolerance levels.

3. Results

3.1. Se depletion and mass extinctions

The overall trend for Se levels observed throughout the Phanerozoic shows that, relative to modern levels, Se dropped dramatically in the oceans below critical thresholds during three mass extinction events at the end of the Ordovician, Devonian, and Triassic (Figs. 2–6). These three key biotic crises are further analysed and discussed in detail below.

3.2. End-Ordovician extinction event

The end-Ordovician extinction was a complex event that commenced ~455 Ma and ended with two pulses, 445 Ma and 443 Ma, which were preceded by south pole glaciations (Harper et al., 2013). Dramatic changes in sea level coupled with tropical ocean cooling possibly played a role in the extinctions (Finnegan et al., 2012), while others suggest euxinia and a sudden drop in oxygen caused the first pulse, with transgression of anoxic water onto continental shelves driving the second pulse (Hammerlund et al., 2012). The Se curve shows a massive drop in Se levels in pyrite from a peak at 523 Ma of 548 ppm Se (geometric mean), or 365 ppt for seawater Se using the concentration factor outlined above (Fig. 3), to lows of around 2 ppm (Se in pyrite) equivalent to c. 1 ppt (seawater Se) by 455 Ma (Fig. 3), which equates to approximately <1% of the level of current Se levels in the modern ocean, well within a Se-deficient zone based on known tolerance levels for many extant marine organisms as discussed above. Selenium levels in pyrite then rise steeply into the Silurian.

The two end-Ordovician extinction pulses thus occur after two prolonged pulses of Se depletion (Fig. 3). The first major extinctions are documented as beginning in the later half of the second Se depleted phase (c. 457–449 Ma) with select families of brachiopods (*Foliomeria* and *Probosciambon* faunas, early virgianid faunas, Fig. 3, labelled A, B) which decline from around 450–448 Ma (Sutcliffe et al., 2001). Extreme Se deficiency in the oceans fluctuated for about 13 Myr before the first major pulse of the extinction took effect, with the second, most severe pulse at the end of the Hirnantian only 2 Ma later (Harper et al., 2013). This extended phases of severe marine Se depletion at the end of Se cycle 1 (Fig. 2) would have made it difficult for

complex organisms with large selenoproteomes to survive, and thus could have affected much of the marine food chain, with those species that were more dependent on Se being the first to succumb. The great Ordovician biodiversification event, which took place throughout the Ordovician, and peaked before the Katian (Servais et al., 2010), was apparently not affected by the Se depletion events at the end of the period.

3.3. Middle–Late Devonian extinction events

The Middle–Late Devonian extinctions fall into two pairs of pulses starting with the Taghanic and Frasnian Crises (House, 2002; McGhee et al., 2013; McGhee, 2014), followed by two events near the Frasnian–Famennian boundary (Kellwasser event; Gereke and Schindler, 2012) and at the end of the Devonian (Hangenberg event; Sallan and Coates, 2010). The Mid-Givetian Taghanic Event (c. 385 Ma) is ranked as the 7th most severe biotic crisis in the Phanerozoic, with some 71 families of marine invertebrates going extinct (McGhee et al., 2013). The Frasnian–Famennian Kellwasser event, dated at 373–374 Ma, saw widespread loss of marine species (13–40% loss at family level, 50–60% of all genera, 72–80% of all marine species lost; McGhee, 2014). The Hangenberg event (c. 359 Ma) saw further extinctions, with some 50% of all vertebrate diversity lost (Sallan and Coates, 2010). The Kellwasser event has been characterised by the spread of oceanic anoxia (Riquier et al., 2006), but may have been restricted to epicontinental shelf seas and not necessarily as widespread as previously thought (George et al., 2014).

Analyses of bio-essential TE abundance (such as Co, Cu, Ni, Mn, Zn, Mo and Cd) through the Devonian show a trend of sequential deficiency at staggered periods between 400 and 350 Ma (Fig. 4A, 5). The sequence of deficiency is Co (Emsian), Mn, Cu, Ni, Zn (Givetian), Mo and Se (Famennian) and Cd (Famennian–Tournasian). The sequential deficiency is most likely related to redox potential and residence times of the respective TE. Co and Mn are the least soluble under oxidised conditions, with short residence times, whereas Se, Mo and Cd are the most soluble with longer residence times (Large et al., 2015a). Cu, Ni and Zn have intermediate residence times. Thus, as global anoxia increased through the Middle to Late Devonian, the TE was drawn down sequentially. Marine organisms not affected by the sequential deficiencies of Co, Cu, Ni and Zn in the Emsian to Givetian, could have been affected by the peak Mo, Se and Cd deficiencies in seawater over the Famennian to Tournasian period. The cycling of Cd, Ni and Zn in the oceans is intimately tied to biogenic cycles (Armouroux et al., 2001), and Cu is associated with micronutrient cycles and a deep water scavenging process (Daniellson et al., 1985). Both Co and Cd can substitute for Zn in diatoms in Zn depleted waters, so it has been suggested that in certain TE-impoorished conditions substitution by other trace metals or metalloenzymes could be a common strategy for phytoplankton

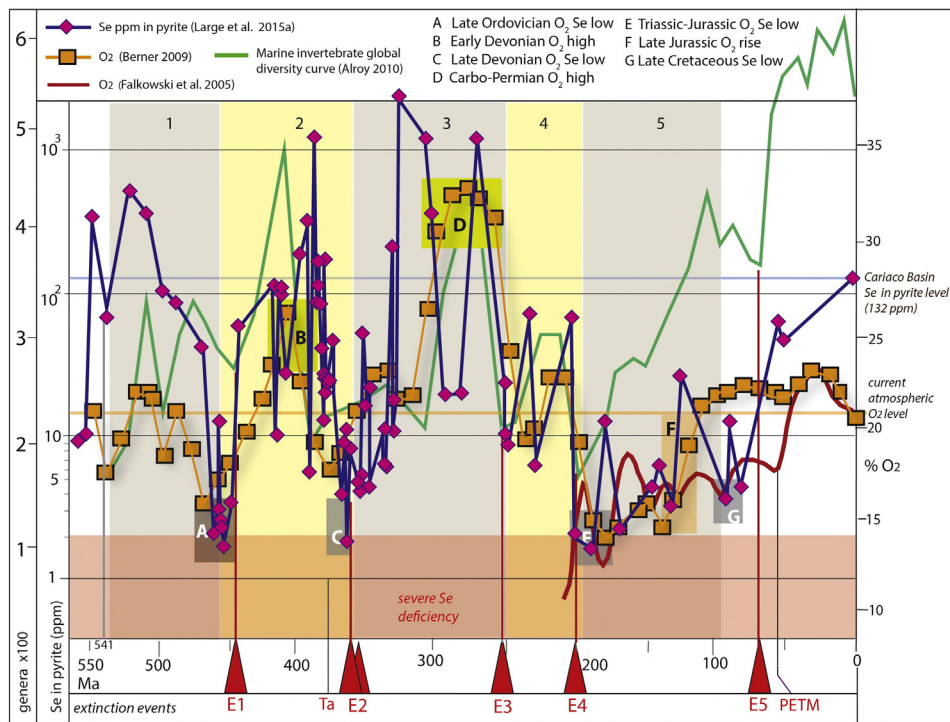


Fig. 2. Phanerozoic time chart showing geometric mean values of Se in pyrite defining five cycles of relative TE enrichment, bracketed by shorter periods of TE depletion (Large et al., 2015a). Three major mass extinction events correlate with extreme Se deficiency preceding times of very low global oxygen (boxes A, C, E). Two models for global oxygen levels (Falkowski et al., 2005; Berner, 2009) are plotted against Alroy's (2010, Fig. 7) marine biodiversity curve using global data. Major times of peak global oxygen labelled in green boxes, peak lows of Se and O₂ in dark boxes. Major mass extinction events: E1, end Ordovician; E2, Frasnian–Famennian; Hangenberg; E3, Permo–Triassic; E4, end Triassic; E5, Cretaceous–Paleogene. Minor biotic crisis: Ta, Taghanic event; PETM, Paleocene–Eocene Thermal Maximum. IUGS time scale, v.2013/01, January 2013. (For interpretation of the references to colour in this figure legend, the reader is referred to the web version of this article.)

survival (Price and Morel, 1990). This strategy may not have been possible at certain critical times based on our data, which shows overlapping periods of peak depletion for many elements.

Another observation arising from the Devonian Se chart (Fig. 4) is the sudden drop at the end of the Emsian, c. 393 Ma. This corresponds

with another series of minor extinction event in the marine realm, where many vertebrate groups (most families of osteostracans, galeaspid, heterostracans, and several placoderm families) went extinct (Long, 1993; Janvier, 1996) followed by two extinction pulses where guilds of invertebrates went extinct in the early and end-Eifelian (lower and upper Kacak events; McGhee et al., 2013).

Se has the longest period of deficiency, reaching its most depleted level at around 367 Ma, just following the Frasnian–Famennian event (Fig. 4A). This was the time leading up to 370 Ma that fish began breathing air (Clack, 2007; Clement and Long, 2010) and tetrapods, the first vertebrates equipped to leave the water and invade land, also appeared (Clack, 2014). Perhaps the collapse of the food chain resulting from the biotic crises at this time was a factor in tetrapods attempting to leave the water and invade land, although complete tetrapod terrestriality was not achieved effectively until the Early Carboniferous (Long and Gordon, 2004).

As SeO_3^{2-} and SeO_4^{2-} are relatively soluble under an oxygenated atmosphere, they were likely drawn down as insoluble HSe^- species through the long span of Frasnian–Famennian anoxia. This pattern could have been reversed by large inputs of oxygen from the rapid increase in terrestrial plant biomass over the Middle–Late Devonian (Algeo et al., 2001; Gibling and Davies, 2012). The evolution of secondary growth in plants saw an increase in heights from around 2 m in the Middle Devonian to large trees up to 20 m by the Late Famennian (Algeo et al., 2001). Land coverage by plants increased from ~10% to ~30% at this time and spread from lowland to also include upland habitats (Gibling and Davies, 2012). Both factors helped significantly increase global plant biomass between the Mid–Late Devonian, and thus, a large source of new atmospheric oxygen. We also note that massive sea floor exhalation from mid-ocean ridges and continental margins occurring as part of the Variscan orogeny from 356 to 345 Ma accounts for further injection of nutrients into the oceans bringing about increased marine photosynthesis and thus more oxygen (Tornos, 2006).

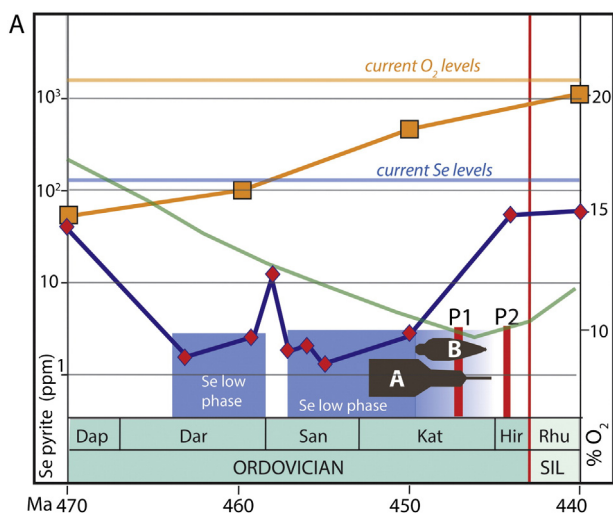


Fig. 3. Mass extinction events at the end Ordovician with modelled levels of global oxygen (orange squares; Berner, 2009) and measured Se in pyrite (red diamonds, blue line) plotted with Alroy's (2010) marine biodiversity curve (green line). Extinction pulses shown in red. The end Ordovician event, with diversity diagrams of major groups of brachiopods (A, B) that begin to decline at around 450 Ma (Sutcliffe et al., 2001) just before the major extinction pulses (P1, P2). (For interpretation of the references to colour in this figure legend, the reader is referred to the web version of this article.)

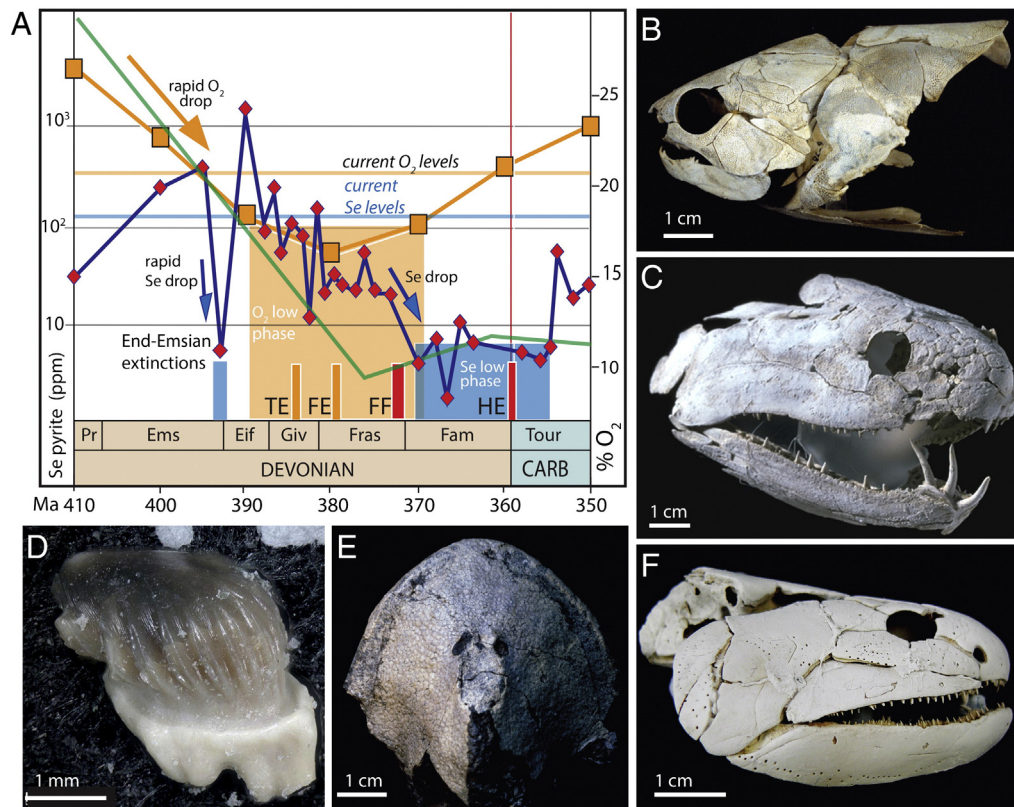


Fig. 4. (A) The Mid–Late Devonian extinction events with measured Se in pyrite curve (red diamonds, blue line), modelled global oxygen (orange squares and line, Berner, 2009) and Alroy's (2010) biodiversity curve (green line). Extinction events in red, minor biotic crisis are in orange (extinction zone as shaded red background): TE, Taghanic event; FE, Frasnian event; FF, Frasnian–Famennian event (Kellwasser); and HE, Hangenberg event (end Devonian). End Emsian extinctions (Long, 1993) are also here defined by a short, rapid Se decline. Examples of major vertebrate extinctions and events related to marine conditions: all placoderms (D), osteostracans (B), and in fact all armoured jawless fishes and many osteichthyan families (e.g. onychodonts, C) went extinct at the end of the Devonian (HE event). From the Taghanic event onwards, fishes began to show adaptations for breathing air (Clement and Long, 2010), as seen here in the large spiracles of the osteolepid *Gogonasus* (F, Long et al., 2006; Clack, 2007). (For interpretation of the references to colour in this figure legend, the reader is referred to the web version of this article.)

3.4. End-Triassic extinction event

Extinctions at the end of the Triassic (c. 201 Ma) include major losses in both marine and terrestrial habitats and are ranked as the second most severe Phanerozoic biodiversity crisis. In the marine realm about 20% of families and up to 50% of genera went extinct, including the iconic conodonts (Onoue et al., 2012). Terrestrial vertebrate extinctions included large archosaurs, except for dinosaurs, which paved the way for niche occupation by the dinosaur radiation in the Jurassic.

The event has been linked to the massive volcanic eruptions of the Central Atlantic Magmatic Province that caused a rapid rise in atmospheric carbon dioxide and methane, with ensuing acidification and localised anoxia driving marine extinctions (Blackburn et al., 2013). Asteroid impacts have been invoked at this time based on the recognition of shocked quartz (Bice et al., 1992), but dismissed as having only localised extinction effects (Onoue et al., 2012). Data from long chain n-alkanes preserved in fossil plants suggest a strong warming effect on land caused by increased greenhouse gases (Ruhl et al., 2011).

Our data imply extremely low Se levels in the ocean between 202 and 190 Ma close to levels at the end of the Ordovician and Late Devonian as pyrite Se levels are about 2 orders of magnitude lower than in modern ocean pyrite, and therefore a similar extinction mechanism could have been operating as during these earlier mass extinctions (Fig. 6). Extremely low levels of Cd at 202–190 Ma are also lower than at any other time in the Phanerozoic.

As mentioned above, the end-Triassic was also a time of increasing CO₂ levels (Royer, 2006) and widespread high fire regimes (Belcher et al., 2010). One model shows O₂ levels rising from around 10% PAL

at 205 Ma to about 17% PAL by 190 Ma (Falkowski et al., 2005), whereas another shows O₂ dropping from high levels at the end of the Triassic (23% PAL: c. 220 Ma) to a peak low at around 180 Ma of 14% PAL, followed by a gradual rise (Berner, 2009). However, despite conflicting estimates of oxygen levels at this time, the rapid decline in marine Se levels is clear (Fig. 6) and might therefore have been a more significant factor in the marine extinctions. Gaseous exchange of Se from phytoplankton to the atmosphere has been proposed as a way in which the biogenic cycle of oceanic Se can directly influence terrestrial Se levels (Armouroux et al., 2001), so could have affected the terrestrial food chain.

4. Discussion

What caused severe Se and other TE depletions in the oceans is not yet resolved, but theoretically explainable. High atmospheric oxygen levels increase oxidative erosion, releasing more Se, Mo, Ni, and other TEs into the oceans (Large et al., 2014, 2015a,b). Increased nutrients in the oceans drive increased biogenic productivity and consequently more burial of organic matter which further fuels increased oxygen production as a positive feedback loop (Large et al., 2015a). As this regime continued, Se levels increased in the ocean. Subsequently, lower atmospheric oxygen or higher sea-level cover of land area meant less erosion due to less terrestrial oxidation, so lower amounts of TEs moved into the oceans. This caused rapid drawdown of Se and certain other TEs, leading to levels falling below critical thresholds necessary for sustaining most marine life. Based on the TE data the periods of minimum Se may have lasted

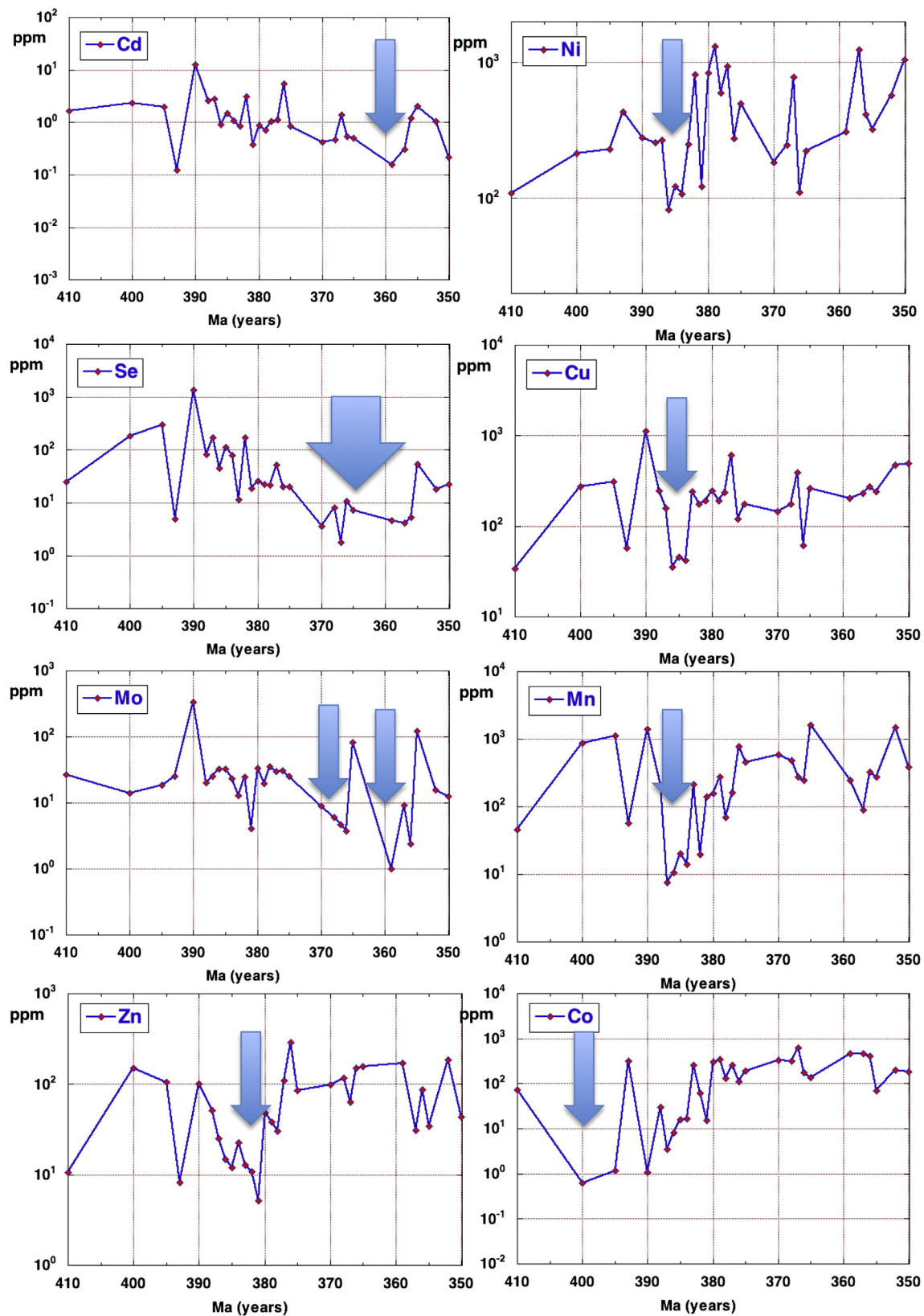


Fig. 5. Patterns of mean trace elements in pyrite through the Devonian. Blue arrows indicate minimum values where TE was likely deficient in the oceans. Trace element minima are shown to be sequential from Co in the Early Devonian to Se, Mo and Cd in the latest Devonian. (For interpretation of the references to colour in this figure legend, the reader is referred to the web version of this article.)

up to 10 Ma before rebound. Because of the low ocean productivity during the Se minima, nutrient TE drawdown would have slowed dramatically; however, nutrient supply related to continental

erosion would be on-going. This resulted in a gradual build-up of TEs in the ocean, activating a rebound of marine life and a consequent positive feedback of increased atmosphere oxygen. Thus, the

upturn in oxygen and Se and recovery from extinction conditions may have been a part of the ocean–atmosphere cycles.

Alternatively, the Se depletion cycles may have been broken by jumps in global oxygen from sudden major increases in plant biomass. In the Silurian, the primary invasion of land plants was widespread (Gibling and Davies, 2012). The Late Devonian saw a massive increase in land plant size from the predominantly mid-sized forms (around 2–3 m) in the Middle Devonian, to an abundance of tree-sized forms up to 20 m by the end Devonian, with plants occupying much larger land areas (Algeo et al., 2001). The end Triassic is also characterised by major increases in global CO₂ associated with high floristic turnover (Belcher et al., 2010). Thus, in each of the three extinction scenarios it was possible that the increase of atmospheric oxygen supplied by increasing plant biomass could have been the significant factor in breaking the anoxia–Se cycle and restoring balance to the marine TE cycle.

The new data also fit well with the current explanation for the mass extinction event at the end of the Permian caused by massive volcanic eruptions (Table 1), where major marine extinctions are not related to anomalous TE levels (Knoll et al., 2007). There are also several Se depletion events prior to the major K–Pg boundary extinctions at 66 Ma. We find no evidence in the fossil record to suggest that these depletions had any major effect on marine ecosystems at the time, although we note that the combination of low Se levels with low oxygen (Falkowski et al., 2005) was only attained during the other three prior mass extinction events that we have discussed (Fig. 2). The global extinction of ichthyosaurs around 93 Ma (Bardet, 1992) might potentially reflect the beginning of changes to the marine food chain caused by such effects or simply be an artefact of poor sampling (Benson et al., 2009).

5. Conclusions

We suggest that depletion of essential TEs (in particular Se) to potentially lethal levels is shown to be highly correlated with, and a likely contributing factor to, at least three mass extinction events in the marine realm, in association with a range of other environmental factors such as increasing/decreasing global oxygen and carbon dioxide levels, euxinia and major eustatic sea level changes in the oceans. Increased atmospheric oxidation increased oxidative erosion, releasing more Se, Mo, Ni, and other TEs into the oceans. Increased nutrients in the oceans drove increased biogenic productivity and consequently more burial of

organic matter which further fuelled increased oxygen production as a positive feedback loop. As this regime continued, Se levels increased in the ocean. Increased global anoxia in the oceans caused rapid draw-down of Se and certain other TEs. Lower atmospheric oxygen or higher sea-level cover of land area meant less erosion due to less terrestrial oxidation, so lower amounts of TEs flowed back into the oceans, leading to levels falling below critical thresholds necessary for a high percentage of marine life. The cycle was broken by sudden changes in oxygen levels, perhaps as result of rapid recovery by increased biomass of plants on land responding to higher CO₂ levels or by invading more land area, as was the case at each of the three mass extinction events.

The new data also fit well with the current explanation for the mass extinction event at the end of the Permian (Table 1), where major marine extinctions are not seen to have been related to anomalous TE levels. We have no Se data across the Cretaceous–Paleogene boundary, so cannot make any comment here.

Our hypothesis is based on a 3.5 billion year history of trace element abundance in the oceans, but now needs further refinement from additional data, not only from pyrite samples filling in temporal gaps in our database, but also on minimal Se and other essential TE requirements across a wider range of living organisms to develop and test models of ecosystem collapse under times of severe TE oceanic depletion.

Acknowledgements

For general discussion, or commenting on sections of the draft MS, we thank Dr. Gavin Prideaux (Flinders University), Prof Peter Ward (University of Adelaide) and Dr Jim Gehling (SA Museum). Analysis of sedimentary pyrite used in this study was completed by Elena Lounejeva, Dan Gregory and Charles Makoundi. JAL's involvement in this research was supported by Flinders University's strategic professor fund. RRL, LD and JAH are supported by the Australian Research Council (DP 150102578) and the University of Tasmania.

References

- Algeo, T.J., Schreckler, S.E., Maynard, J.B., 2001. Effects of Middle to late Devonian spread of vascular land plants and weathering regimes. In: Gensel, P.G., Edwards, D. (Eds.), *Plants Invade the Land*. Columbia University Press, NY, pp. 213–237.
- Alroy, J., 2010. Geographical, environmental and intrinsic biotic controls on Phanerozoic marine diversification. *Palaeontology* 53, 1211–1235.
- Armouroux, D., Liss, P.S., Tessier, E., Hamren-Larson, M., Donard, O.F.X., 2001. Role of oceans as biogenic sources of selenium. *Earth and Planetary Science Letters* 189, 277–283.
- Bardet, N., 1992. Stratigraphic evidence for the extinction of ichthyosaurs. *Terra Nova* 4, 649–656.
- Belcher, C.M., Mander, L., Rein, G., Jervis, F.X., Haworth, M., Hesselbo, S.P., Glasspool, I.J., McElwain, J.C., 2010. Increased fire activity at the Triassic/Jurassic boundary in Greenland due to climate-driven floral change. *Nature Geoscience* 3, 426–429.
- Benson, R.B.J., Butler, R.J., Lindgren, J., Smith, A.S., 2009. Mesozoic marine tetrapod diversity: mass extinctions and temporal heterogeneity in geological megabiases affecting vertebrates. *Proceedings of the Royal Society of London B* 272, 829–834.
- Benton, M., Twitchett, J., 2003. How to kill (almost) all life: the end Permian extinction event. *Trends in Ecology and Evolution* 18, 358–365.
- Berner, R.A., 2009. Phanerozoic atmospheric oxygen: new results using the GEOCARBSULF model. *American Journal of Science* 309, 603–606.
- Bice, D.M., Newton, C.R., McCaughley, S.M., et al., 1992. Shocked quartz at the Triassic–Jurassic boundary in Italy. *Science* 255, 443–446.
- Blackburn, T.J., Olsen, P.E., Bowring, S.A., et al., 2013. Zircon U–Pb geochronology links the end-Triassic extinction with the Central Atlantic Magmatic Province. *Science* <http://dx.doi.org/10.1126/science.12134204>.
- Brezinski, D.K., Blaine Cecil, C., Skema, V.W., Stamm, R., 2008. Late Devonian glacial deposits from the eastern United States signal an end of the mid–Paleozoic warm period. *Palaeogeography, Palaeoclimatology, Palaeoecology* 268, 143–151.
- Charlet, L., Kang, M., Bardelli, F., Kirsch, R., Géhin, A., Grenèche, J.M., Chen, F., 2012. Nano-composite pyrite–greigite reactivity toward Se(IV)/Se(VI). *Environmental Science & Technology* 46, 4869–4876.
- Clack, J.A., 2007. Devonian climate change, breathing, and the origin of the tetrapod stem group. *Integrative and Comparative Biology* 47, 510–523.
- Clack, J.A., 2014. *Gaining Ground*. Indian University Press.
- Clement, A., Long, J.A., 2010. Air-breathing adaptation in a marine Devonian lungfish. *Biology Letters* 6, 509–512.
- Cutter, G.A., 1989. The estuarine behaviour of selenium in San Francisco Bay. *Estuarine, Coastal and Shelf Science* 28, 13–34.

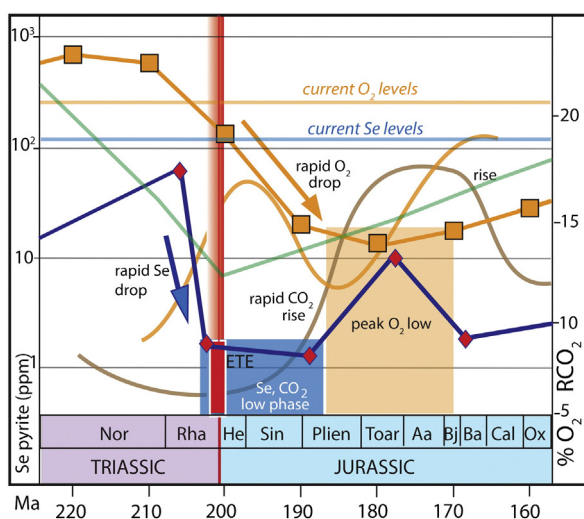


Fig. 6. The end Triassic extinction event (ETE) showing two modelled oxygen curves (orange squares and lines, Berner, 2009; orange curved line, Falkowski et al., 2005), measured Se in pyrite curve (red diamonds, blue line), modelled carbon dioxide levels (brown curve, Ruhl et al., 2011) and Alroy's (2010) biodiversity curve (green line). Note the sudden decline in Se here marks the timing of the main extinction event well before oxygen reaches its peak low. (For interpretation of the references to colour in this figure legend, the reader is referred to the web version of this article.)

- Cutter, G.A., Bruland, K.W., 1984. The marine biogeochemistry of selenium: a re-evaluation. *Limnology & Oceanography* 29, 1179–1192.
- Cutter, G.A., Cutter, L.S., 1995. Behavior of dissolved antimony, arsenic, and selenium in the Atlantic Ocean. *Marine Chemistry* 49, 295–306.
- Daniellson, L.-G., Magnusson, B., Westerlund, S., 1985. Cadmium, copper, iron, nickel and zinc in the north-east Atlantic Ocean. *Marine Chemistry* 17, 23–41.
- Diener, A., Neumann, T., Kramar, U., Schild, D., 2012. Structure of selenium incorporated in pyrite and mackinawite as determined by XAFS analyses. *Journal of Contaminant Hydrology* 133, 30–39.
- Doblin, M.A., Blackburn, S.I., Hallegraeff, G.M., 1999. Comparative study of selenium requirements of three phytoplankton species: *Gymnodinium catenatum*, *Alexandrium minutum* (Dinophyta) and *Chaetoceros cf. tenuissimus* (Bacillariophyta). *Journal of Plankton Research* 21, 1153–1169.
- Eisler, R., 2000. Selenium. *Handbook of Chemical Risk Assessment: Health Hazards to Humans, Plants and Animals* vol. 3. Lewis Publishers, CRC Press, Boca Raton, FL, pp. 1649–1705.
- Falkowski, P.G., Katz, M.E., Milligan, A.J., Fennel, K., Cramer, B.S., Aubry, M.P., Berner, R.A., Novacek, M.J., Zapol, W.M., 2005. The rise of oxygen over the past 205 million years and the evolution of large placental mammals. *Science* 309, 2202–2204.
- Fan, A.M., Kizer, K.W., 1990. Selenium – nutritional, toxicologic and clinical aspects. *Western Journal of Medicine* 153, 160–167.
- Finnegan, S., Heim, N.A., Peters, S.E., Fischer, W.W., 2012. Climate change and selective signature of the late Ordovician mass extinction. *Proceedings of the National Academy of Sciences of the United States of America* 109, 6829–6834.
- Fordyce, F., 2007. Selenium geochemistry and health. *Ambio* 36, 94–97.
- George, A.D., Chow, N., Trinajstić, K.M., 2014. Oxidic facies and the Late Devonian mass extinction, Canning Basin, Australia. *Geology* <http://dx.doi.org/10.1130/G35249.1>.
- Gereke, M., Schindler, E., 2012. “Time-specific facies” and biological crisis – the Kellwasser event interval near the Frasnian/Famennian boundary (Late Devonian). *Palaeogeography, Palaeoclimatology, Palaeoecology* 367–368, 19–29.
- Gibling, M.R., Davies, N.S., 2012. Palaeozoic landscapes shaped by plant evolution. *Nature Geoscience* 5, 99–105.
- Hamilton, S.J., 2004. Review of selenium toxicity in the aquatic food chain. *Science of the Total Environment* 326, 1–31.
- Hammerlund, E.U., Dahl, T.W., Harper, D.A.T., et al., 2012. A sulfidic driver for the end Ordovician mass extinction. *Earth and Planetary Science Letters* 331–332, 128–139.
- Harper, D.A.T., Hammerlund, E.U., Rasmussen, C.M.O., 2013. End Ordovician extinctions: a coincidence of causes. *Gondwana Research* 25, 1294–1307.
- Harrison, P.J., Yu, P.W., Thompson, P.A., et al., 1988. Survey of selenium requirements in marine phytoplankton. *Marine Ecology Progress Series* 47, 89–96.
- Herring, J.R., 1991. Selenium geochemistry—a conspectus. *US Geological Survey Circular* 1064, 7–23.
- Hilton, J.W., Hodson, P.V., Slinger, S.J., 1980. The requirements and toxicity of selenium in rainbow trout (*Salmo gairdneri*). *Journal of Nutrition* 110, 2527–2535.
- House, M., 2002. Strength, timing, setting and cause of mid Palaeozoic extinctions. *Palaeogeography, Palaeoclimatology, Palaeoecology* 181, 5–25.
- Janvier, P., 1996. *Early Vertebrates*. Oxford University Press (393 pp.).
- Keller, M., Guillard, R.R.L., Provasoli, L., Pintner, I.J., 1984. Nutrition of some marine ultraplankton clones from the Sargasso Sea. *Eos* 65, 898.
- Kharkar, D.P., Turekian, K.K., Bertine, K.K., 1968. Stream supply of dissolved silver, molybdenum, antimony, selenium, chromium, cobalt, rubidium and cesium to the oceans. *Geochimica et Cosmochimica Acta* 32, 285–298.
- Kim, H.-J., Sakakura, Y., Maruyama, I., Nakamura, T., Takiyama, K., Fujiki, H., Hagiwara, A., 2014. Feeding effect of selenium enriched rotifers on larval growth and development in red sea bream *Pagrus major*. *Aquaculture* 432, 273–277.
- Klasing, K.C., 1998. *Comparative Avian Nutrition*. Oxford University Press, New York.
- Knoll, A.H., Bambach, R.K., Payne, J.L., Pruss, S., Fischer, W.W., 2007. Paleophysiology and end-Permian mass extinction. *Earth and Planetary Science Letters* 256, 295–313.
- Kulp, T.R., Pratt, L.M., 2004. Speciation and weathering of selenium in Upper Cretaceous chalk and shale from South Dakota and Wyoming, USA. *Geochimica et Cosmochimica Acta* 68, 3687–3701.
- Large, R.R., Halpin, J.A., Danyushevsky, L.V., Maslennikov, V.V., Bull, S.W., Long, J.A., Gregory, D.D., Lounejeva, E., Lyons, T.W., Sack, P.J., McGoldrick, P.J., Calver, C.R., 2014. Trace element content of sedimentary pyrite as a new proxy for deep-time ocean–atmosphere evolution. *Earth Planet Science Letters* 389, 209–220.
- Large, R.R., Halpin, J.A., Lounejeva, E., Danyushevsky, L.V., Maslennikov, V.V., Lottermoser, B.G., Sack, P.J., Haines, P.W., Long, J.A., Makoundi, C., 2015a. Selenium and cobalt in sedimentary pyrite reveal Phanerozoic cycles of Earth’s oxygenation. *Gondwana Research* <http://dx.doi.org/10.1016/j.gr.2015.06.004>.
- Large, R.R., Gregory, D.D., Steadman, J.A., Tomkins, A.G., Lounejeva, E., Danyushevsky, L.V., Halpin, J.A., Maslennikov, V.V., Sack, P.J., Mukherjee, I., Berry, R., Hickman, A., 2015b. *Gold in the oceans through time*. *Earth and Planetary Science Letters* 428, 139–150.
- Lin, Y.H., Shai, S.Y., 2005. Dietary selenium requirements of juvenile grouper, *Epinephelus malabaricus*. *Aquaculture* 250, 356–363.
- Lobanov, A.V., Fomenko, D.E., Zhang, Y., Sengupta, A., Hatfield, D.L., Gladyshev, V.N., 2007. Evolutionary dynamics of eukaryotic selenoproteomes: large selenoproteomes may associate with aquatic life and small with terrestrial life. *Genome Biology* 8, R198. <http://dx.doi.org/10.1186/gb-2007-8-9-r198>.
- Long, J.A., 1993. Early–Middle Palaeozoic vertebrate extinction events. In: Long, J. (Ed.), *Palaeozoic Vertebrate Biostratigraphy and Biogeography*. Belhaven Press, London, pp. 54–63.
- Long, J.A., Gordon, M., 2004. The greatest step in vertebrate history: a paleobiological review of the fish–tetrapod transition. *Physiological and Biochemical Zoology* 77 (5), 700–719.
- Long, J.A., Young, G.C., Holland, T., Senden, T.J., Fitzgerald, E.M.G., 2006. An exceptional Devonian fish from Australia sheds light on tetrapod origins. *Nature* 444, 199–202.
- McGhee Jr., G.R., 2014. *When the Invasion of Land Failed. The Legacy of the Devonian Extinctions*. Columbia University Press, New York (317 pp.).
- McGhee Jr., G.R., Clapham, M.E., Sheehan, P.M., et al., 2013. A new ecological-severity ranking of major Phanerozoic biodiversity crises. *Palaeogeography, Palaeoclimatology, Palaeoecology* 370, 260–270.
- Mertz, W., 1957. The essential trace elements. *Science* 213, 1332–1338.
- Mitchell, K., Mason, P.R.D., Van Cappellan, P., Johnson, T.M., Gill, B.C., Owens, J.D., Diaz, J., Ingall, E.D., Reichart, G.-J., Lyons, T.W., 2012. Selenium as paleo-oceanographic proxy: a first assessment. *Geochimica et Cosmochimica Acta* 89, 302–317.
- Nakaguchi, Y., Mitsuhashi, Y., Kitahata, K., Fujita, A., Sumiyoshi, A., Kawai, Y., 2008. Selenium speciation in the eastern tropical and subtropical South Pacific Ocean. *Science and Technology* 21, 25–33.
- Neal, R.H., Sposito, G., Holtzclaw, K.M., Traina, S.J., 1987. Selenite adsorption on alluvial soils: I. Soil composition and pH effects. *Soil Science Society of America Journal* 51, 1161–1165.
- Onoue, T.S., Sato, H., Nakamura, T., et al., 2012. Deep-sea record of impact apparently unrelated to mass extinction in the Late Triassic. *Proceedings of the National Academy of Sciences of the United States of America* 109, 19134–19139.
- Plant, J.A., Korre, A., Reeder, S., Smith, B., Voulboulis, N., 2005. Chemicals in the environment: implications for global sustainability. *Transactions of the Institution of Mining and Metallurgy Section B: Applied Earth Science* 114, B65–B97.
- Price, N.M., Harrison, P.J., 1988. Specific selenium-containing macromolecules in the marine diatom *Thalassiosira pseudonana*. *Plant Physiology* 86, 192–199.
- Price, N.N., Morel, F.M.M., 1990. Cadmium and cobalt substitute for zinc in a marine diatom. *Nature* 344, 658–660.
- Price, N.M., Thompson, P.A., Harrison, P.J., 1987. Selenium: an essential element for growth of the coastal marine diatom *Thalassiosira pseudonana* (Bacillariophyceae). *Journal of Phycology* 23, 1–9.
- Riquier, L., Tribouillard, N., Averbuch, O., Devleeschouwer, X., Riboulleau, A., 2006. The Late Frasnian Kellwasser horizons of the Harz Mountains (Germany): two oxygen-deficient periods resulting from different mechanisms. *Chemical Geology* 233 (1–2), 137–155.
- Royer, D.L., 2006. CO₂-forced climate thresholds during the Phanerozoic. *Geochimica et Cosmochimica Acta* 70, 5665–5675.
- Ruhl, M., Bonis, N.R., Reichart, G.-J., Sinninghe Damste, J.S., Kurschener, W.M., 2011. Atmospheric carbon injection linked to end-Triassic mass extinction. *Science* 333, 430–433.
- Ryser, A.L., Strawn, D.G., Marcus, M.A., Johnson-Maynard, J.L., Gunter, M.E., Möller, G., 2005. Micro-spectroscopic investigation of selenium-bearing minerals from the Western US phosphate resource area. *Geochemical Transactions* 6, 1–11.
- Sallan, L.C., Coates, M.C., 2010. End-Devonian extinction and a bottleneck in the early evolution of modern jawed vertebrates. *Proceedings of the National Academy of Sciences of the United States of America* 107, 10131–10136.
- Servais, T., Owen, A.W., Harper, D.A.T., Kröger, B., Munnecke, A., 2010. The great Ordovician biodiversification event (GOBE): the palaeoecological dimension. *Palaeogeography, Palaeoclimatology, Palaeoecology* 294, 99–119.
- Shrift, A., 1964. A selenium cycle in nature? *Nature* 201, 1304–1305.
- Spallholz, J.E., 1994. On the nature of selenium toxicity and carcinostatic activity. *Free Radical Biology and Medicine* 17, 45–64.
- Sugimura, Y., Suzuki, Y., Miyake, Y., 1976. The content of selenium and its chemical form in sea water. *Journal of the Oceanographical Society of Japan* 32, 235–241.
- Sutcliffe, O.E., Harper, D.A.T., Salem, A., Whittington, R.J., Craig, J., 2001. The development of an atypical Hirnantia-brachiopod fauna and the onset of glaciation in the late Ordovician of Gondwana. *Transactions of the Royal Society of Edinburgh: Earth Sciences* 92, 1–14.
- Thisse, C., Degraeve, A., Kryukov, G.V., et al., 2003. Spatial and temporal expression patterns of selenoprotein genes during embryogenesis in zebrafish. *Gene Expression Patterns* 3, 525–532.
- Tornos, F., 2006. Environment of formation and styles of volcanogenic massive sulfides: the Iberian Pyrite Belt. *Ore Geology Reviews* 28, 259–307.
- Wang, W., Mai, K.M., Zhang, W., 2012. Dietary selenium requirement and its toxicity in juvenile abalone *Haliotis discus hannai* Ino. *Aquaculture* 330–333, 42–46.
- Wheeler, A.E., Zingaro, R.A., Irgolic, K., Bottino, N.R., 1982. The effect of selenate, selenite and sulphate on the growth of six unicellular green algae. *Journal of Experimental Marine Biology and Ecology* 57, 181–194.